Electronic supplementary information

Catalysis By the JmjC Histone Demethylase KDM4A Integrates Substrate Dynamics, Correlated Motions and Molecular Orbital Control

Rajeev Ramanan,[a] Shobhit S. Chaturvedi,[a] Nicolai Lehnert,[b] Christopher J. Schofield,[c] Tatyana G. Karabencheva-Christova,[a,*] and Christo Z. Christov.[a,*]

[a] Department of Chemistry, Michigan Technological University, Houghton, Michigan 49931, USA.

[b] Department of Chemistry, University of Michigan, Ann Arbor, MI, 48019, USA

[c] The Chemistry Research Laboratory, Mansfield Road, University of Oxford, OX1 5JJ, United Kingdom.

* E-mail: tatyanak.@mtu.edu, christov@mtu.edu.

List of Figures

List of Tables

Other Information

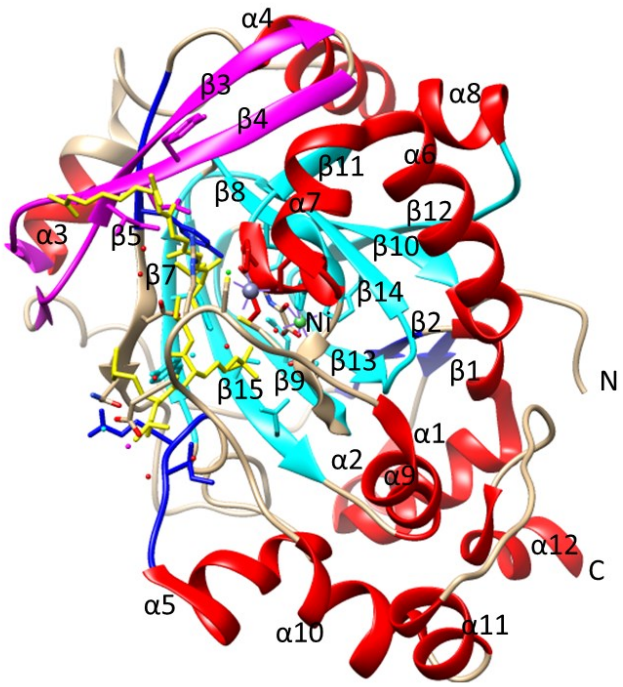

Figure S1. Secondary elements of the KDM4A.Ni.N-oxalylglycine.H3(7-12)K9me3 complex structure (based on PDB: 2oq6).

Methods

1. System Setup and MD Simulation: Crystal structures of the catalytic domain of KDM4A bound to the H3(7-12)K9me3 natural substrate (PDB ID: 2OQ6)[1] or to a cyclic peptide substrate analogue / inhibitor (PDB ID: 5LY1)[1] were used. The Ni in the crystal structure was replaced with Fe(II) and the 2OG analogue N-oxalylglycine (NOG) was modified to 2OG by replacing its NH with a methylene group. A crystal structure of PHF8 complexed with an H3(1-14)K4me3K9me2 substrate fragment (PDB ID: 3KV4)[1] was treated similarly to the KDM4 structures (NOG was modified to 2OG). Missing hydrogen atoms and counter ions for neutralization were added with the Leap module of Amber16.[2] Parameters for non-standard ligands /residues such as 2OG and the

substrate were developed using Antechamber as implemented in Amber. Parameters for the metal ion (Fe(II)) at the active site were prepared using the Metal Center Parameter Builder (MCPB.py).[3] Parameters were generated for both the Fe(III)-superoxo and Fe(IV)-oxo complexes for the respective MD simulations. The Fe(II) is high spin (S=2, M=5) in its ground state, as shown in previous studies[4] and is coordinated with: 2OG (bidentate), two histidine residues and one glutamic acid (monodentate), consistent with crystallographic studies[1] (Fig. 2). 2OG was replaced with mono-chelated succinate in the ferryl intermediate. The parameters generated using the MCPB tool are reported to be accurate for describing mononuclear non-heme iron centers and iron-sulfur Rieske clusters.[5] The zinc-binding region in KDM4A was described using the Zinc AMBER force field (ZAFF).[6]

The FF14SB force field was employed in MD simulations.[7] The protein was immersed in a rectangular box with TIP3P (transferable intermolecular potential with 3 points model) water molecules.[8] The edge of the box was 10 Å from the protein surface. MD simulations were performed under periodic boundary conditions. The Particle Mesh Ewald (PME) method with a direct space and Van der Waals (vdW) cut-off of 8 Å was used to calculate long-range electrostatic interactions.[9] Initial energy minimizations were done in two steps, i.e. the steepest descent (5000 steps), followed by the conjugate gradient method (5000 steps). In the first minimization, only the solvent and ions were allowed to minimize while the solute molecules were restrained using a potential of 500 kcal/mol $Å^2$. This was followed by full minimization of the entire protein and solvents with steepest descent (5000 steps) and conjugate gradient (5000 steps). Energy minimization steps were performed with the CPU version of the Amber16 code (SANDER). The minimized system was annealed from 0 to 300 K in an NVT ensemble for 300 ps. A subsequent run for 750 ps in the NPT ensemble at a constant temperature of 300 K and pressure of 1.0 atm.

was carried out using Langevin-thermostat[10] and Barendsen barostat[11] with a pressure relaxation time of 1 ps. The systems were then equilibrated for ~3 ns. All bonds with hydrogen were constrained with the SHAKE algorithm.[12] The final production MD run for 1μs (1000 ns) was performed in an NPT ensemble. The target pressure was set at 1 bar with a constant pressure coupling of 2ps. The final productive molecular dynamics simulations were conducted using the GPU version of the Amber16 code (PMEMD).[2] Detailed analyses of the trajectories were performed with the inbuilt amber analyzing tool CPPTRAJ,[13] Visual Molecular Dynamics (VMD),[14] and other software packages that enable protein structure analysis such as UCSF Chimera,[15] and R (Bio3D).[16] Principal Component Analysis (PCA) and dynamics cross-correlation analysis (DCCA) were added to the analysis with the Bio3D package.[16] The PCA analysis helps to understand the details of protein motion while DCCA analysis provides all correlated motions of residues during the dynamics.

2. QM/MM Calculations: The Quantum Mechanical (QM) region in the hybrid Quantum Mechanical/Molecular Mechanics (QM/MM) calculation included the Fe, O_2, His276, His188, Glu190, tri methylated lysine (M3L) of H3(7-12)K9me3 substrate, 2OG, and two water molecules as shown in Fig. 2 for the Fe(III)-superoxo complex. For the Fe(IV)-oxo complex, 2OG and O_2 were replaced with succinate and an oxygen atom, respectively. The consistency of the results was validated by calculations with an expanded QM region that additionally included Lys241, Tyr177, and Asn290. QM/MM calculations were performed with the ChemShell suite of programs.[17,18] Turbomole was used for the QM region,[19] while DL_POLY for the MM region.[20] Amber force fields generated for the MD simulation were used in the QM/MM step. The polarizing effect of the protein on the QM region was accounted with the electronic embedding scheme.[21] All geometries were optimized using the B3LYP[22] density functional theory with the def2-SVP (Split

valence polarization) basis set (B1) which can reproduce accurate barriers and electronic structure for Fe metal containing systems.[23,24] Transition states were optimized in two steps. First, a relaxed potential energy surface (adiabatic mapping) scan was performed by gradually changing a reaction coordinate[24] The highest energy point on the scanned surface was reoptimized for the TS. The DL-find optimizer algorithm implemented in Chemshell was used for reactant optimization and scanning.[25] The HDLC (hybrid delocalized coordinates) optimizer was used for the final TS optimization.[26] The initial guesstimate of the TS obtained from potential energy surface (PES) scanning was very close to the final TS, showing only small geometric and energy differences. Frequency calculations were performed to verify the first order and second-order saddle points. Further single points were calculated to refine the energies with higher basis sets at the B3LYP/def2-TZVP level of theory (B2).[23,24]

QM/MM results on Oxygen Activation by KDM4A with H3(7-12)K9me3 Substrate

We carried out QM/MM reaction modeling studies to investigate the detailed mechanism of oxygen activation by the catalytic domain of KDM4A (**RC1** to **IM2**, Figure 2). Following binding of O_2 to give a superoxide complex (**RC1**), a succinyl peroxide intermediate (**IM1**) is formed, concomitant with decarboxylation of 2OG; homolytic O-O bond-breaking of **IM1** generates a ferryl intermediate (**IM2**) (Figure 2). The energies of possible spin states of **RC1**, i.e. singlet, triplet, quintet and septet states were calculated. Calculations were done by single point calculations on the quintet optimized geometry at the B2 level of theory. Both the singlet and triplet energies of **RC1** are higher than that of the quintet state of **RC1**, by 19.8 and 23.8 kcal/mol, respectively. The septet energy of **RC1** is close to that of the quintet state by -0.5 kcal/mol.

However, the subsequent potential septet of **TS1** is higher in energy than that for the quintet state of **TS1** by 2.3 kcal/mol. Thus, the possibility of O_2 activation through possible spin states other than the quintet state seems unlikely. The decarboxylation step on going from **RC1** to **IM1** has a barrier 12.1 kcal/mol at the QM(B2+ZPE)/MM level of theory. The stabilizing interactions of the C5 carboxylate oxygens of 2OG with Tyr132 and Lys206, as well as the 2OG O1 oxygen with Asn198, remains conserved at the decarboxylation transition state (**TS1** in Figure S2). **RC1** and **TS1** are stabilized by interactions with Tyr177, Lys241, and Asn290. Overall, the O_2 activation mechanism for KDM4A resembles that established for other 2OG oxygenases.[4]

The results of QM/MM reaction modelling studies concerning the mechanism of oxygen reaction of the KDM4A.Fe.superoxo.H3(7-12)K9me3 complex (**RC1**) are summarized in Figure S2. In the first step, the distal oxygen (Od) of the superoxo complex (**RC1**) approaches the C2 ketone carbonyl of 2OG. C2-Od bond formation, as shown in Figure S2a, causes 2OG C1-C2 carbonyl bond elongation, eventually leading to decarboxylation and formation of a succinyl peroxide intermediate **IM1**, for which there is experimental evidence in some cases.[27] This observation implies that in the case of KDM4A, 2OG decarboxylation is a near concerted process with C2–Od bond formation. Non-heme enzymes generally have a high spin quintet ground state for their iron cofactor.[4a,b] Transition state (**TS1**) manifests near simultaneous C2–Od bond formation and CO_2 departure. The barrier for decarboxylation to give **IM1** is 12.1 kcal/mol at the QM(B2+ZPE)/MM level of theory, which together with the reasonable thermodynamic stability of the following intermediate, **IM1**, suggests efficient oxygen activation.

These observations agree with previous studies on model complexes and some other 2OG dependent oxygenases.[4a,b] Decarboxylation is the rate-determining step (RDS) during oxygen activation from **RC1** to give **IM1**. Exothermic (-36.4 kcal/mol) decarboxylation of **RC1** leads to

the formation of succinyl peroxide intermediate **IM1**. The transition state, **TS1** has elongated Fe-Op and C1-C2 bonds (2.07 and 1.73 Å, respectively) relative to **RC1**.

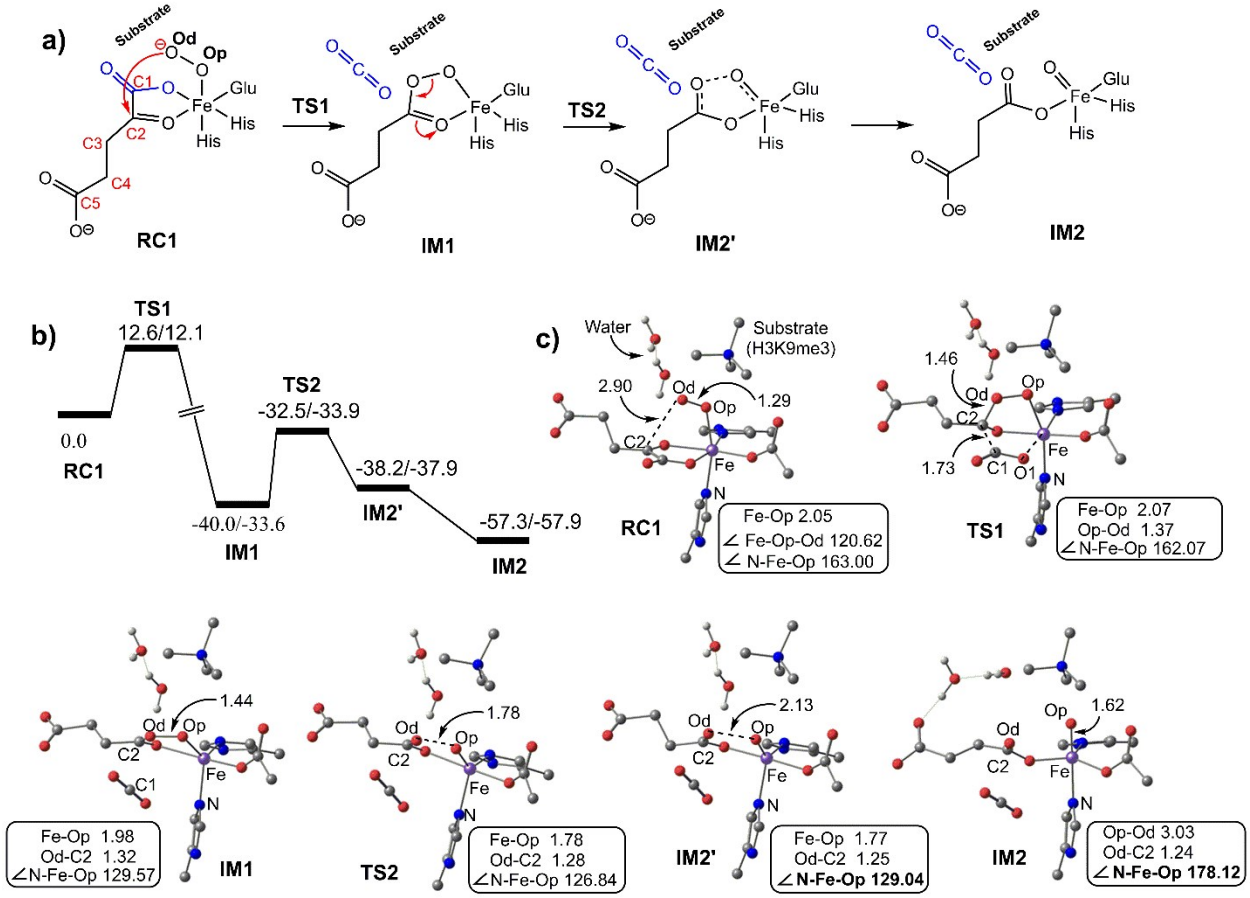

Figure S2. The QM/MM modeled oxygen activation step in KDM4A catalysis. (**a**) Mechanism for 2OG dependent oxygen activation. (**b**) Potential energy profile (in kcal/mol) at the QM(B2)/MM followed by QM(B2+ZPE)/MM level of theory. (**c**) The QM region of QM(B1)/MM optimized geometries.

A network of hydrogen bonds formed by water molecules and residues with polar side chains (Tyr177, Lys241, Asn198, and Tyr132) around 2OG contribute to O_2 activation (Figure

S5). Figure S1c shows the interactions of two water molecules that were included in the QM region. O-O homolysis of the peroxide **IM1** has a barrier of 7.5 kcal/mol at the QM(B2)/MM level of theory. The addition of zero point energy (ZPE) correction predicts barrier-less homolysis. After homolysis, the resulting transient intermediate, **IM2'**, has a partial bond (2.13 Å) between the oxygen (Op-Od) atoms; the Fe-Op bond distance in **IM2'** is 1.77 Å. Rearrangement of **IM2'** gives the ferryl-oxo intermediate **IM2** [Fe(IV)-oxo], which has an Fe-O distance of 1.61 Å and which is stabilized by around -57 kcal/mol relative to the initial reactant complex **RC1**. CO_2 is assumed to exit the active site. The results suggest that following after the first decarboxylation step, the low energy barrier to homolysis of **IM1** and succeeding exothermic steps may minimize side reactions sometimes associated with radical intermediates (Figure S2).

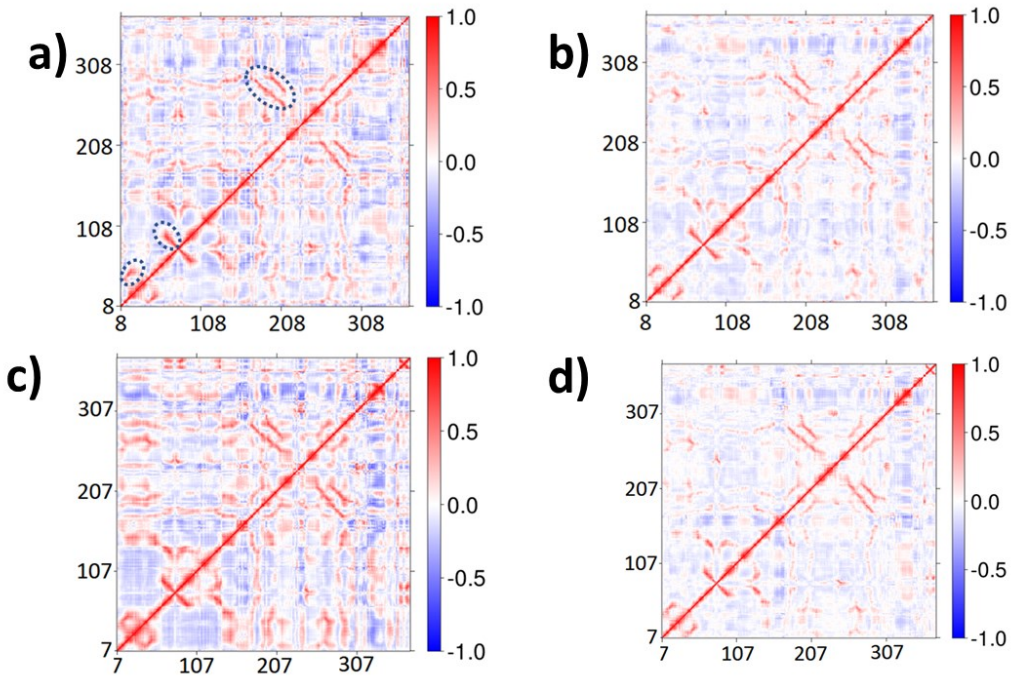

Figure S3. Dynamic cross correlation diagram of the (**a)** Fe(III)-O_2/2OG, (**RC1**) (**b)** Fe(IV)-oxo/succinate (**IM2**) complexes with H3(7-12)K9me3 substrate, (**c)** the **RC1** (and) the **(d) IM2** complex with the cyclic peptide CP2. Note that in addition to those described in the main text, there are correlated motions between residues 47-50 (belonging to β2 and β3) and 16-22 (β1 and the following loop) and residues 81-98 (β5) with 63-77 (loop between β2 and β3). β1 and β2 are located relatively distant from the active site. The DSBH β3 helps form the substrate-binding cavity as does β5.

Details of Correlated motions in the CP2(R6Kme3) bound complex

The correlated motions involving Lys 241 and Asn290, which are predicted to be important in orienting the substrate, may differ in the Fe(III)-superoxo complex (**RC1**) and the Fe(IV)-oxo complex (**IM2**). Long-range correlated interactions in the Fe(III)-superoxo (**RC1**) complex therefore could help promote oxygen activation. In the Fe(IV)-oxo (**IM2**) complex specific

correlated motions might regulate hydrogen atom transfer. In the Fe(III)-superoxo complex (**RC1**), Lys241 motion correlates with residues 83-84 in β4 (which extends DSBH) and Ala186 which is close to the Fe-coordinating His188. In the Fe(IV)-oxo complex (**IM2**), correlation of Lys241 with the β4 strand is decreased while the correlation of Lys241 with Ala186 persists. In the Fe(III)-O_2 (**RC1**) complex, Asn290 shows additional correlations with residues; 31-45 (α2, 3.10H1, and β2), 148-155 (the loop connecting β5 to α5), 175 (on β7), 188-198 (β9 with the preceding loop), 269-273 (β13), 356-358 (Zn-binding region; Fe and succinate binding). It is interesting that α2, α5, 3.10H1, and β2 are distant from the substrate binding pocket. β5 is close to the Zn binding region, while β7, β9, and β13 belong to the DSBH. The cross correlations of Asn290 in the Fe(IV)-oxo complex (**IM2**) were reduced to residues 194-196 that belong to β9 and the preceding loop. Thus, correlated motions of Asn290 may be important in the reaction of Fe(III)-O_2 (**RC1**) to give **IM1** then **IM2**.

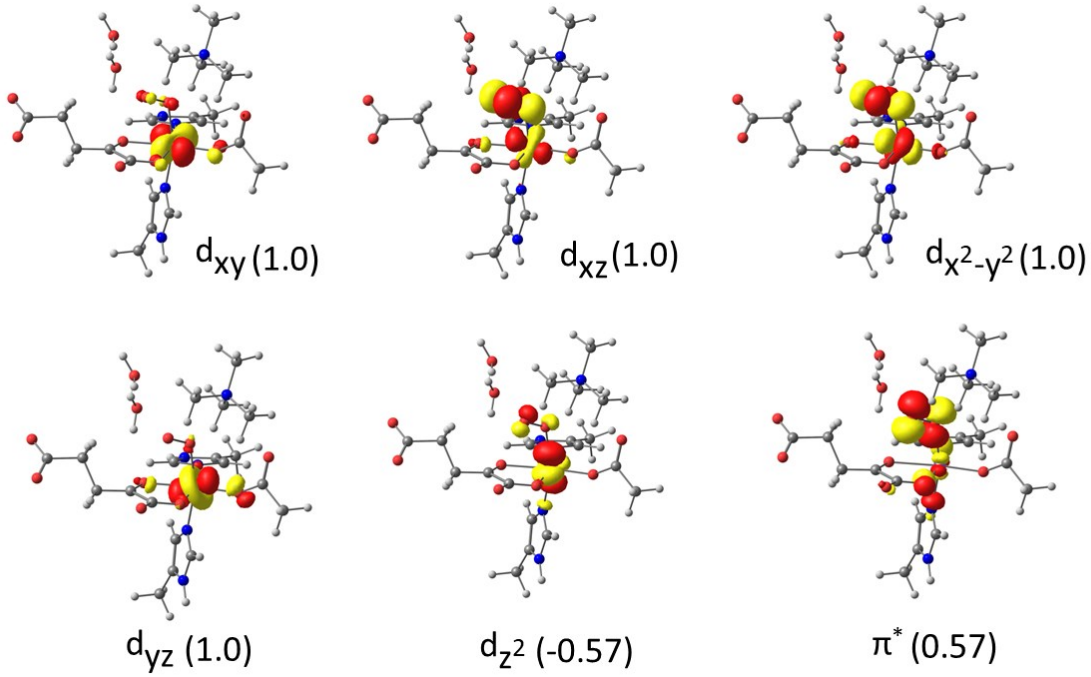

Figure S4. Spin Natural Orbitals (SNO) for the Fe-superoxide complex (**RC1**).

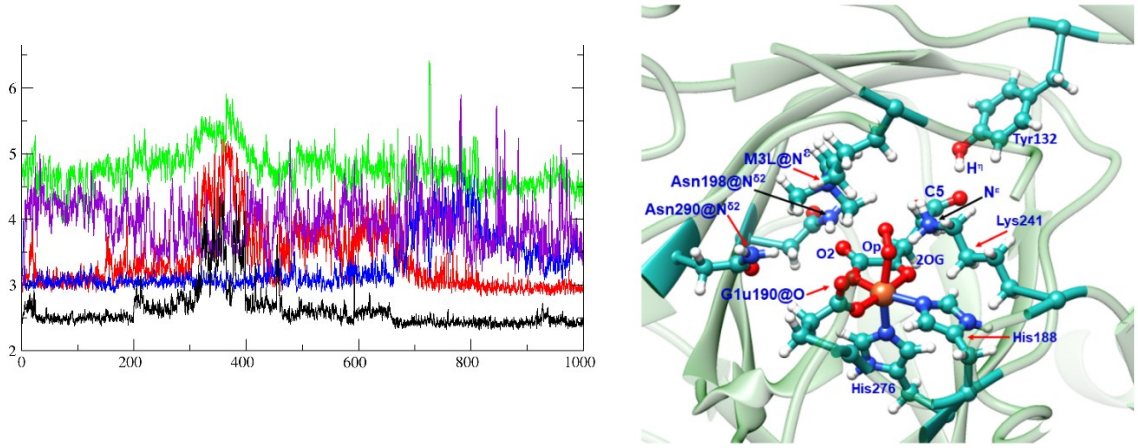

Figure S5. Distance plots for the Fe(III)-O_2.H3(7-12)K9me3 complex. Color code: 2OG@C5-Tyr132@H^{η} distance in black; dioxygen Op-Lys241@N^{ε} in violet; G1u190@O(noncoordinating)-M3L@N^{ε} in green; G1u190@O(non-coordinating O)-Asn290@$N^{\delta 2}$ in blue; Asn198@$N^{\delta 2}$-O2@2OG in red.

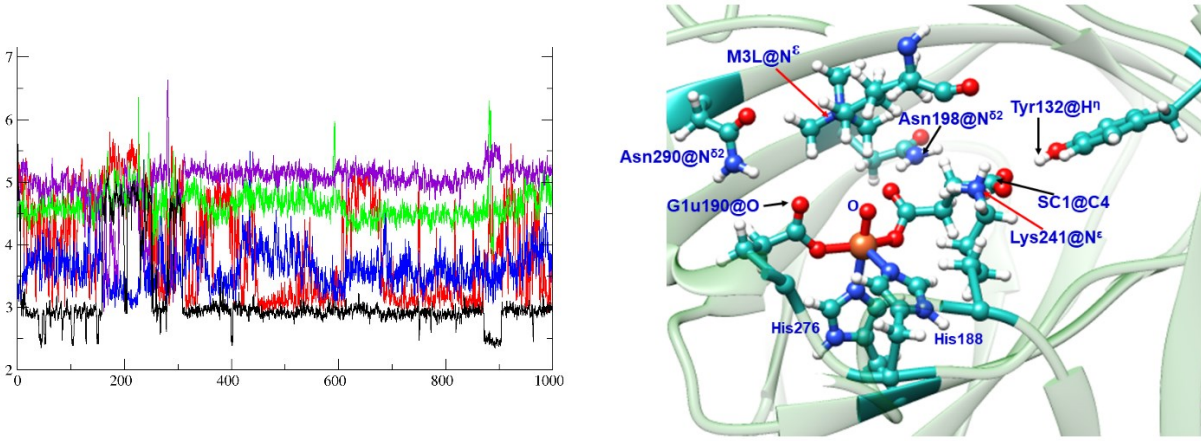

Figure S6. Distance plots for the Fe(IV)-oxo.succinate.H3(7-12)K9me3 complex. Color code: SC1@C4-Tyr132@H^{η} in black; O-Lys241@N^{ε} in violet; G1u190@O(noncoordinating)-M3L@N^{ε} in green; G1u190@O(non-coordinating O)-Asn290@$N^{\delta 2}$ in blue; Asn198@$N^{\delta 2}$-O2@SC1 in red. SC, succinate.

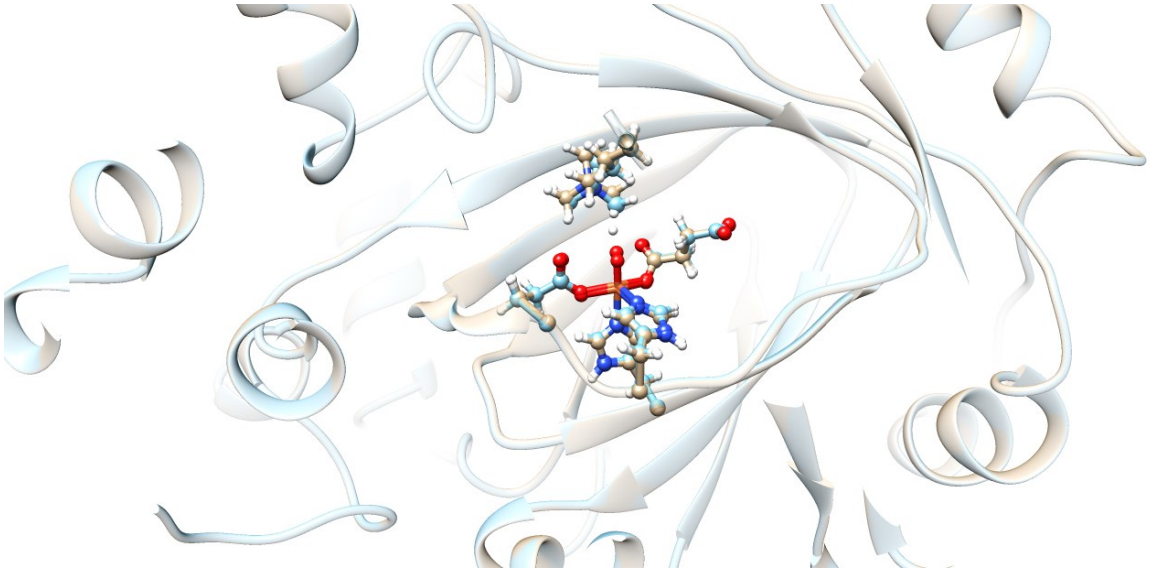

Figure S7. Superimposed geometries of the optimized reactant with the HAT transition state for the KDM4A.Fe(IV)-oxo.succinate.H3(7-12)K9me3 (**IM2**) complex.

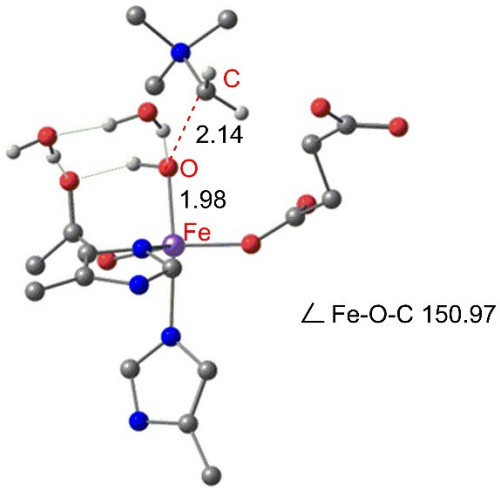

Figure S8. The QM region of QM(B1)/MM optimized geometry of the rebound step for the KDM4A.Fe(IV)-oxo.H3(7-12)K9me3 complex.

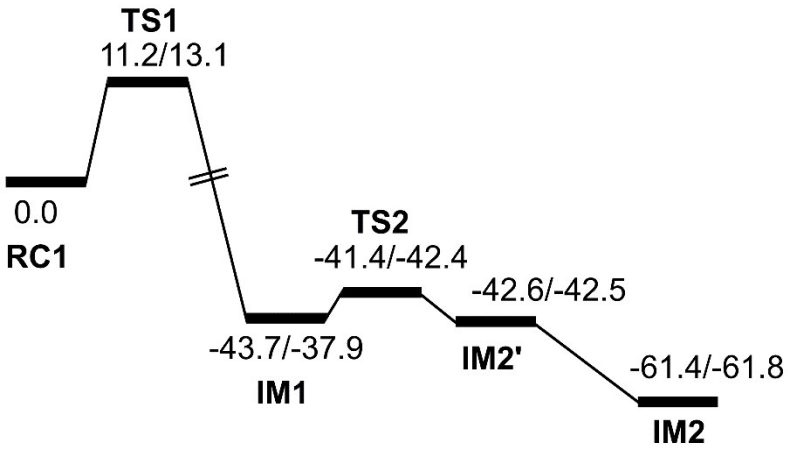

Figure S9. Potential energy profile (in kcal/mol) at the QM(B2)/MM level of theory followed by the QM(B2+ZPE)/MM level of theory for O_2 activation in the presence of the cyclicpeptide, CP2, bound complex.

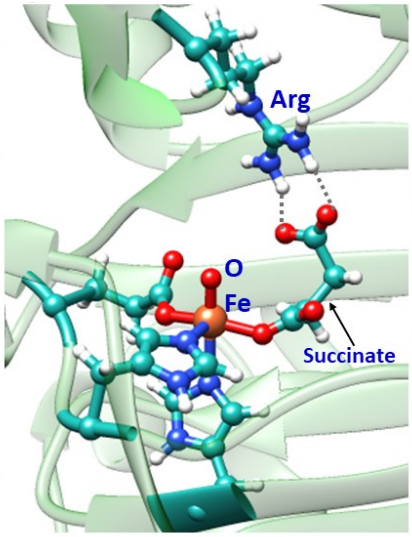

Figure S10. The hydrogen-bonding interaction of CP2-Arg at the active site of KDM4A.

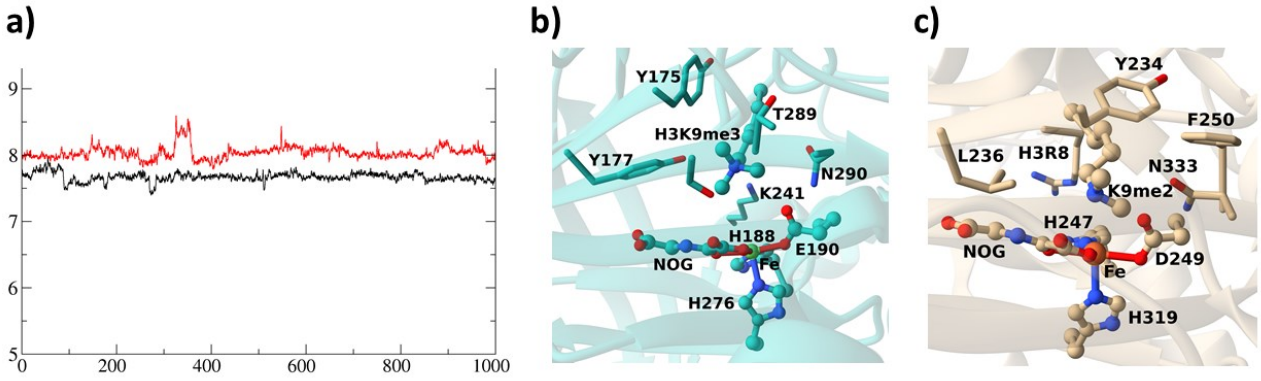

Figure S11. Comparison of active site details of KDM4A and PHF8 enzymes. **a)** Radii of gyration of the Fe(IV)-oxo active site in KDM4A (red) and PHF8 (black). The *y*-axis is labeled with the radius of gyration in Å and *x*-axis with time in ns. **b)** Active site geometry of KDM4A (based PDB: 2OQ6) and **c)** PHF8 (based PDB ID: 3KV4).

Table S1. Mulliken spin densities of intermediates and transition states for the O_2 activation pathway in Figure S1.

	Fe	**Op**	**Od**
RC1	4.2	-0.2	-0.5
TS1	4.2	-0.1	-0.2
IM1	3.8	0.1	0.0
TS2	3.9	0.1	-0.2
IM2'	4.1	-0.2	-0.3
IM2	3.1	0.6	0.1

Table S2. Mulliken charges of intermediates and transition states in the O_2 activation pathway in Figure S1.

	Fe	**Op**	**Od**
RC1	0.7	-0.2	-0.2
TS1	0.6	-0.4	-0.1
IM1	0.7	-0.5	-0.2
TS2	0.7	-0.5	-0.3
IM2'	0.8	-0.6	-0.4
IM2	0.6	-0.5	-0.5

Table S3. Mulliken spin densities of intermediates and transition states for the hydroxylation step shown in Figure 6.

	Fe	**O**	**Substrate**	**Rest**
IM2	3.2	0.6	0	0.2
TS_HAT	4.0	0.1	-0.5	0.4
IM3	4.2	0.3	-1.0	0.5
TS_Rb	4.1	0.1	-0.6	0.4
PD	3.8	0.0	0.0	0.2

Table S4. Mulliken charges of intermediates and transition states in the hydroxylation step shown in Figure 6.

	Fe	O	Substrate	Rest
IM2	0.7	-0.6	0.9	-1.1
TS_HAT	0.8	-0.6	1.1	-1.3
IM3	0.7	-0.7	1.3	-1.3
TS_Rb	0.7	-0.7	1.4	-1.4
PD	0.8	-0.4	1.4	-1.8

Table S5. Mulliken Spin Densities of multiple hydrogen atom transfer (HAT) trajectories shown in Figure 6.

Entry[a]	Barrier		Fe	O	Substrate	Rest
2	23.2	**IM2**	3.1	0.6	0.0	0.3
		TS_HAT	4.0	0.1	-0.5	0.4
3	27.3	**IM2**	3.1	0.7	0.0	0.2
		TS_HAT	4.0	0.0	-0.4	0.4
4	28.3	**IM2**	3.1	0.6	0.0	0.3
		TS_HAT	4.0	0.1	-0.5	0.4
5	26.1	**IM2**	3.1	0.6	0.0	0.3
		TS_HAT	4.0	0.0	-0.5	0.5

-*a*- entry **1** is in **Table S3**.

Table S6. Mulliken charges of multiple hydrogen atom transfer (HAT) shown in Figure 6.

Entry[a]	Barrier		Fe	O	Substrate	Rest
2	23.2	**IM2**	0.6	-0.5	0.9	-1.0
		TS_HAT	0.7	-0.6	1.1	-1.2
3	27.3	**IM2**	0.7	-0.5	0.9	-1.1
		TS_HAT	0.8	-0.6	1.1	-1.3
4	28.3	**IM2**	0.6	-0.5	0.9	-1.0
		TS_HAT	0.8	-0.7	1.1	-1.2
5	26.1	**IM2**	0.7	-0.5	0.9	-1.1
		TS_HAT	0.8	-0.6	1.1	-1.3

-*a*- entry **1** is in **Table S3**.

Table S7. Mulliken Spin Densities of multiple hydrogen atom transfer (HAT) trajectories shown in Figure 9.

Entry	Barrier		Fe	O	Substrate	Rest
1	20.6	**IM2**	3.2	0.5	0.0	0.3
		TS_HAT	4.1	-0.2	-0.4	0.5
2	19.8	**IM2**	3.1	0.6	0.0	0.3
		TS_HAT	4.0	-0.1	-0.4	0.5
3	21.1	**IM2**	3.1	0.6	0.0	0.3
		TS_HAT	4.0	-0.1	-0.4	0.5
4	31.8	**IM2**	3.1	0.6	0.0	0.3
		TS_HAT	3.9	0.1	-0.4	0.4
5	29.0	**IM2**	3.1	0.6	0.0	0.3
		TS_HAT	4.1	-0.1	-0.4	0.4

Table S8. Mulliken charges of multiple hydrogen atom transfer (HAT) trajectories shown in Figure 9.

Entry	Barrier		Fe	O	Substrate	Rest
1	20.6	**IM2**	0.8	-0.6	0.9	-1.1
		TS_HAT	0.8	-0.6	1.0	-1.3
2	19.8	**IM2**	0.7	-0.5	0.9	-1.1
		TS_HAT	0.8	-0.7	1.0	-1.1
3	21.1	**IM2**	0.7	-0.5	0.9	-1.1
		TS_HAT	0.8	-0.7	1.1	-1.2
4	31.8	**IM2**	0.6	-0.4	0.9	-1.1
		TS_HAT	0.8	-0.6	1.1	-1.3
5	29.0	**IM2**	0.6	-0.5	0.9	-1.0
		TS_HAT	0.8	-0.8	1.1	-1.1

The Cartesian Coordinates of the Optimized QM Region of QM/MM Geometry. QM/MM energies at the QM(B2)/MM level of theory are given in Hartree.

O_2 Activation step

RC1
QM/MM Energy = -3208.879920

6	39.044965236	29.442057704	33.081114753
1	37.966791579	29.627519915	33.199621246
1	39.148522467	28.372432397	32.853650802
6	39.741122662	29.792340070	34.352999685
7	40.960447503	29.270094905	34.733870591
1	41.574269193	28.666730890	34.173626351
6	41.333164587	29.842784050	35.889577081
1	42.260693594	29.628467385	36.409762429
7	40.412079821	30.709294274	36.288680816
6	39.407572918	30.682817626	35.346684580
1	38.529774745	31.317201651	35.430794774
6	37.685431920	35.208161851	37.506341151
1	38.426175000	35.668934908	36.840520219
1	37.722318966	35.694229824	38.492512967
6	38.018960158	33.735581600	37.741828493
8	39.156522119	33.352642881	37.265643027
8	37.240136779	33.006023178	38.364789397
6	44.487228174	34.023071011	33.404281876
1	45.492111189	33.811124097	33.810405835
1	44.514810951	35.072777165	33.069626453
6	43.443634271	33.872553167	34.475357721
7	43.120098222	34.942584639	35.290296119
1	43.411569739	35.922627709	35.228390789
6	42.268045284	34.530464996	36.244295561
1	41.881545366	35.181983992	37.024843085
7	42.004897916	33.240276670	36.101151009
6	42.727082073	32.815197026	35.000847414
1	42.689935201	31.789526975	34.645626803
26	40.755704380	32.307497314	37.618278242
6	42.562974498	33.138705510	39.688427911
6	43.266827749	31.871678436	39.116613285
6	44.482324876	30.000609344	40.315005303
6	45.855291663	29.562055514	40.891717941
8	42.994554354	33.700196147	40.693581845
8	41.536294343	33.499037015	39.010019900
8	42.688961959	31.315032681	38.177004669
8	46.553321588	30.472064187	41.395904725
6	44.559586924	31.405035052	39.681497340
8	46.134045003	28.344865342	40.818690692
1	43.755274479	30.015549325	41.144865695
1	44.128541595	29.248669709	39.598488676
1	45.286029365	31.379379338	38.849542343
1	44.927318661	32.114168148	40.431631597
8	40.074476489	31.087375146	39.113603574
8	40.740978203	30.954565658	40.205434539
6	36.360523184	30.737372503	43.346037492
1	36.147225202	31.017104180	44.387297818
1	36.839921508	29.749951109	43.336729386

TS1
QM/MM Energy = -3208.859902

6	39.097245779	29.399493427	33.073377732
1	38.019473889	29.578674584	33.203593108
1	39.204067985	28.331387648	32.838915300
6	39.800203000	29.747278886	34.342027867
7	41.042662645	29.260780761	34.699077372
1	41.666692132	28.681423464	34.124453931
6	41.405106218	29.818723540	35.864225681
1	42.349390940	29.639721821	36.368000544
7	40.456143389	30.640557091	36.292825354
6	39.444490614	30.602082476	35.358670084
1	38.548842346	31.207435034	35.464473233
6	37.796247557	35.089935271	37.507393013
1	38.547846725	35.483206769	36.810779949
1	37.888691362	35.605427790	38.474928651
6	38.044468121	33.607396646	37.788722853
8	39.143310309	33.125696121	37.317805209
8	37.222371373	32.952358816	38.440450049
6	44.496083288	34.000997054	33.401407427
1	45.496138048	33.782953939	33.815786361
1	44.532329035	35.051427318	33.069621801
6	43.442513452	33.854313639	34.463255992
7	43.118092455	34.923947021	35.279519313
1	43.421532543	35.900659254	35.227483229
6	42.252531771	34.515422010	36.221511094
1	41.870917196	35.163212525	37.006757298
7	41.979140399	33.227901246	36.068639259
6	42.711923008	32.800939832	34.975317887
1	42.673512492	31.777406885	34.615202424
26	40.847179251	32.225230482	37.601179017
6	42.301834876	33.322721702	39.808208055
6	42.625564604	31.637789760	39.557733784
6	44.291323280	29.793252271	40.221596030
6	45.685150250	29.502464271	40.843290099
8	42.825396914	33.885308038	40.754572391
8	41.485399430	33.707233639	38.941289676
8	42.592648059	31.429388323	38.275826748
8	46.324484697	30.477271609	41.300898888
6	43.846607244	31.243073576	40.382513259
8	46.055894704	28.306394685	40.809441113
1	43.562748709	29.082286835	40.643420091
1	44.377186045	29.560886831	39.151102513
1	44.671514860	31.897509636	40.066759010
1	43.647435294	31.496482284	41.433483845
8	40.351817306	31.176760126	39.313262547
8	41.389237917	31.201856701	40.204940901
6	36.401165003	30.706844479	43.336081614
1	36.172978910	31.010972482	44.367189829
1	36.863155887	29.711563734	43.359233400

7	37.390519994	31.711851603	42.817533758	7	37.457960825	31.653970143	42.810933389
6	38.595066481	31.632296921	43.713249084	6	38.624847068	31.588349608	43.755122843
6	36.862468432	33.119526841	42.795552445	6	36.946379577	33.066184641	42.726752920
6	37.823928248	31.344541419	41.423312408	6	37.942481817	31.237764891	41.446958735
1	36.509651657	33.381184104	43.801423804	1	36.569554246	33.364542707	43.713529633
1	37.671709126	33.795151480	42.490419773	1	37.772322718	33.722127645	42.423438649
1	36.040750824	33.167412122	42.062686929	1	36.142900470	33.100570780	41.971514881
1	38.142782121	30.292504483	41.441573034	1	38.230986549	30.177413363	41.505672571
1	36.973661543	31.497868188	40.747062297	1	37.129321803	31.386635533	40.726076984
1	38.655109842	31.994739171	41.135113620	1	38.799086599	31.858848454	41.163403388
1	38.961748066	30.596447405	43.716893724	1	38.985858466	30.550876010	43.795561960
1	39.378298118	32.306762070	43.327697753	1	39.422780805	32.256243894	43.389744008
1	38.294772093	31.910922300	44.731952268	1	38.285714150	31.888516623	44.755196188
8	40.872546135	28.045562875	41.303495116	8	40.957323452	28.057263508	41.258504456
1	40.925384012	27.253673242	41.883745389	1	40.981871339	27.253360647	41.826131533
1	41.020075989	28.825758501	41.875320225	1	41.113651873	28.818642035	41.853705272
8	41.599776642	28.171551755	38.737758544	8	41.605438140	28.144508766	38.653932735
1	41.549866565	28.057796818	39.718334009	1	41.571459389	28.045969358	39.634777223
1	42.117535866	28.983601766	38.635537983	1	42.162769545	28.926207376	38.527689067
1	36.693164506	35.418326776	37.107212863	1	36.807028633	35.339127013	37.123444168
1	39.412874957	29.976720679	32.205417737	1	39.452078863	29.940033011	32.195893964
1	44.367880268	33.447752654	32.486222956	1	44.380733613	33.428441447	32.481112987
1	35.431728078	30.669258401	42.779674148	1	35.479264653	30.643280968	42.758044636

IM1

QM/MM Energy = -3208.943626

6	38.989559711	29.397889597	33.030925725
1	37.909437158	29.584348613	33.126516738
1	39.092290272	28.338031600	32.761700656
6	39.643674952	29.674567291	34.340601448
7	40.886442149	29.190853369	34.694584573
1	41.542752253	28.674357900	34.097268831
6	41.191239439	29.653979396	35.918596860
1	42.127954619	29.450740486	36.426545370
7	40.206858237	30.404918484	36.394066227
6	39.232044216	30.422888677	35.419560833
1	38.317853084	30.998431706	35.539920844
6	37.611744427	35.230268622	37.535777101
1	38.358537925	35.701309358	36.882717172
1	37.635869004	35.706065804	38.527418912
6	37.947613439	33.744246015	37.738567788
8	39.052547166	33.365042668	37.238630487
8	37.151255311	33.024387672	38.376019517
6	44.426725455	33.972770718	33.556315716
1	45.424554210	33.753297327	33.976219731
1	44.452146426	35.034424515	33.262168690
6	43.356687110	33.777797477	34.595426043
7	42.899456022	34.851372330	35.337983752
1	43.150814056	35.842664312	35.272227150
6	42.025192917	34.407657763	36.257364504
1	41.529792612	35.061314085	36.970150272
7	41.880348002	33.095297047	36.171797548
6	42.702705629	32.687445817	35.136288378
1	42.768161743	31.648270348	34.826059306
26	40.601821192	32.095915475	37.583454622
6	43.261831469	34.316476760	40.209867705
6	42.639638650	31.239386423	39.571213336

TS2

QM/MM Energy = -3208.931694

6	38.988335433	29.396992705	33.056926765
1	37.906813889	29.577858011	33.145913904
1	39.099334145	28.335503059	32.796910745
6	39.632428898	29.687694210	34.368949775
7	40.867744878	29.198678752	34.745150787
1	41.525485628	28.668957811	34.160070772
6	41.160597711	29.668290042	35.967933166
1	42.087124065	29.461267875	36.492976483
7	40.172550554	30.433141840	36.420649193
6	39.211202110	30.451988885	35.431510565
1	38.306494776	31.044187821	35.533777366
6	37.674068257	35.155965718	37.461276755
1	38.407760325	35.608657105	36.781185833
1	37.755528141	35.620057467	38.455985423
6	37.959084652	33.655783709	37.632764163
8	39.000366474	33.218488161	37.034920075
8	37.181447763	32.970143913	38.321434201
6	44.402347556	33.982056959	33.622787311
1	45.402541680	33.767851787	34.039641932
1	44.422639831	35.043428037	33.327587323
6	43.341067216	33.788819694	34.671668769
7	42.897167097	34.866983250	35.416071682
1	43.148042067	35.858148366	35.339356808
6	42.035067602	34.432941291	36.349702108
1	41.557296076	35.091720636	37.069808080
7	41.886069371	33.120375255	36.272526480
6	42.693458050	32.702803662	35.227372086
1	42.754783322	31.661820910	34.922762453
26	40.586505696	32.093889028	37.635853457
6	43.287485775	34.317818854	40.255168781
6	42.622444189	31.299749888	39.609950497

6	44.432099800	29.615831823	40.306137578	6	44.416831873	29.605067882	40.278820078
6	45.857838255	29.451129008	40.884817443	6	45.844558573	29.415685483	40.850428621
8	43.385649584	34.272691687	41.367736641	8	43.392539879	34.285237459	41.415052978
8	43.158273307	34.357709346	39.055931397	8	43.212638681	34.363001934	39.098864230
8	42.365349407	30.803861386	38.452040375	8	42.328844697	30.878759864	38.465302763
8	46.400550609	30.477041491	41.358602068	8	46.398626356	30.427480231	41.341272455
6	43.943858867	31.061280204	40.291576170	6	43.971479676	31.061306901	40.252676959
8	46.336562253	28.296849836	40.812490460	8	46.312496721	28.257273982	40.766666038
1	43.739716763	28.961864609	40.861890479	1	43.718663954	28.980071133	40.860835151
1	44.446505148	29.235018994	39.280632070	1	44.401482309	29.204443567	39.261520130
1	44.693143572	31.664375582	39.748158100	1	44.702290607	31.636083205	39.656254093
1	43.876010089	31.477614188	41.304841655	1	43.978148563	31.490552064	41.262606802
8	40.536587025	32.251472768	39.559937643	8	40.375747511	32.434064515	39.369098943
8	41.771117727	31.976486075	40.249434717	8	41.824165174	32.020126815	40.313145784
6	36.350779645	30.670711728	43.270054878	6	36.368115163	30.663349951	43.262889379
1	36.110751899	30.989034550	44.294019147	1	36.128879918	30.980605524	44.287372908
1	36.794749324	29.667807258	43.311664090	1	36.808834868	29.658941904	43.303051842
7	37.433760703	31.591050629	42.756772526	7	37.454849363	31.580574221	42.752666656
6	38.574245065	31.499754747	43.731390508	6	38.593526136	31.483152960	43.729398574
6	36.954896732	33.013836544	42.656809488	6	36.982174274	33.005521746	42.654210080
6	37.936431156	31.161632399	41.401894229	6	37.956699994	31.153844042	41.396967795
1	36.564314841	33.323429307	43.634866641	1	36.585597720	33.313481267	43.630381885
1	37.802731328	33.648304862	42.369216174	1	37.835269247	33.636679918	42.374924293
1	36.168804892	33.065189296	41.883715686	1	36.201797368	33.062215622	41.875855483
1	38.204612323	30.096383991	41.476286982	1	38.246917028	30.094750876	41.474547984
1	37.137571608	31.317347672	40.665818581	1	37.147129470	31.286796227	40.668027791
1	38.806372608	31.770759667	41.118498660	1	38.809466877	31.781448926	41.102093160
1	38.922680539	30.457865478	43.768829238	1	38.933690633	30.438668896	43.770010292
1	39.384386302	32.168429734	43.398355712	1	39.408394439	32.145849095	43.395755658
1	38.209846738	31.789787690	44.725551461	1	38.228840618	31.778264882	44.721993020
8	40.911087246	28.023079960	41.310962437	8	40.908935119	28.009565461	41.308791900
1	40.931988583	27.208583123	41.864395499	1	40.935246304	27.198510213	41.866861496
1	41.099605884	28.768154240	41.917116946	1	41.108741145	28.758454897	41.907500309
8	41.473770972	28.032612262	38.684690840	8	41.493848126	28.089282955	38.692070941
1	41.516488684	27.936901952	39.662190139	1	41.534078551	27.963679358	39.666506606
1	41.965226704	28.853885923	38.515744431	1	41.964013544	28.930659149	38.553948948
1	36.626896607	35.447419205	37.122270485	1	36.679636074	35.401473390	37.088586612
1	39.383240142	29.961707598	32.185235297	1	39.380407636	29.955966025	32.207282404
1	44.332324584	33.436287198	32.612207020	1	44.310871198	33.445795280	32.678264782
1	35.434210544	30.609893789	42.683309976	1	35.451386447	30.605975930	42.676046981

IM2'
QM/MM Energy = -3208.940826

6	38.944925960	29.439361154	33.068552953
1	37.866208949	29.639539959	33.148690751
1	39.042483845	28.374574316	32.817944620
6	39.591013079	29.730401804	34.379973310
7	40.814828412	29.212348014	34.754552918
1	41.459983216	28.665856292	34.170766286
6	41.130568225	29.685837391	35.967568119
1	42.057611786	29.467048427	36.485482148
7	40.165824759	30.483348934	36.419580286
6	39.196644687	30.517046090	35.436911295
1	38.307383334	31.131139962	35.540497805
6	37.711722218	35.128929904	37.462880210
1	38.444195195	35.573526017	36.776326727
1	37.805028815	35.597047739	38.454739755

IM2
QM/MM Energy = -3208.971165

6	38.928090974	29.394914440	33.000292221
1	37.844608944	29.571630923	33.066476409
1	39.051567881	28.332765249	32.753249092
6	39.547865691	29.710417129	34.316780915
7	40.761198769	29.215665887	34.746956160
1	41.430462566	28.664308020	34.196996988
6	41.043999563	29.749898334	35.949568975
1	41.951161888	29.557187633	36.516999103
7	40.062857043	30.558030190	36.321090277
6	39.119013638	30.540832263	35.325036282
1	38.206454378	31.126554842	35.385954818
6	37.559622061	35.332765218	37.532955798
1	38.304396170	35.810057479	36.883181711
1	37.549701850	35.838522664	38.509079803

6	37.991727485	33.631893584	37.648882383	6	37.944558012	33.876841768	37.808232427
8	39.064194013	33.197919507	37.092667595	8	39.165967372	33.608428510	37.474308110
8	37.198938537	32.941666139	38.308521610	8	37.142970936	33.093236738	38.321171915
6	44.394958574	33.990296333	33.635588352	6	44.211289327	33.997047608	33.782778723
1	45.396776442	33.782991622	34.051895571	1	45.192704268	33.810932927	34.254358421
1	44.411357587	35.050243893	33.334513295	1	44.215826276	35.063668283	33.503635872
6	43.336523615	33.801866014	34.688965250	6	43.100483637	33.765213410	34.773010414
7	42.894343683	34.885746652	35.426594747	7	42.690112899	34.808061194	35.583183550
1	43.144952513	35.876574821	35.341279642	1	42.987881868	35.790379599	35.568980263
6	42.037885392	34.460731685	36.368553608	6	41.755958703	34.361759129	36.438430442
1	41.567834895	35.125125977	37.088587273	1	41.274130811	34.990651729	37.180946018
7	41.890266265	33.147202477	36.301397993	7	41.526433713	33.072110225	36.246881296
6	42.694282889	32.719424548	35.257046409	6	42.363082512	32.682505846	35.213035060
1	42.758224673	31.675378230	34.964824106	1	42.381258269	31.667882964	34.826723630
26	40.646365766	32.096190319	37.696468557	26	40.313761937	32.059572158	37.716199010
6	43.315128783	34.223084522	40.264667285	6	43.289961166	34.151520612	40.375779854
6	42.857790531	31.230238012	39.364586130	6	42.335535836	31.239910938	39.642123960
6	44.478720242	29.610102855	40.438746491	6	44.614521015	30.687366449	40.654440837
6	45.949979555	29.404088268	40.867587252	6	45.609836543	29.585176596	41.062729840
8	43.433900204	34.209560058	41.422876043	8	43.446759369	34.129113385	41.530159597
8	43.225061741	34.274020637	39.108875248	8	43.157913218	34.202037698	39.224562010
8	42.336364348	30.946065468	38.224886797	8	41.833791665	31.804033946	40.623847729
8	46.525935221	30.422472955	41.320606840	8	45.256671526	28.374410954	41.034356012
6	44.309896406	30.893197539	39.619566769	6	43.456276077	30.229252879	39.780151500
8	46.426411956	28.251546374	40.752494529	8	46.734435788	29.995185420	41.449032195
1	43.888456253	29.716737955	41.360402441	1	44.221681040	31.129837212	41.585774528
1	44.096600181	28.726197427	39.912033928	1	45.198519048	31.478900052	40.158339542
1	44.834452393	30.824364681	38.659144326	1	43.807893293	29.958231364	38.778591856
1	44.770740505	31.700683164	40.207167981	1	42.987215528	29.337428725	40.216257917
8	40.382177607	32.417635620	39.413978169	8	39.416909282	31.338196028	38.852805991
8	42.215590701	31.775891242	40.291844770	8	41.975650867	31.467730533	38.417679166
6	36.395615161	30.643849643	43.278376645	6	36.475754907	30.670582810	43.365438754
1	36.156450609	30.972724683	44.299243634	1	36.261756828	30.944283829	44.408446070
1	36.826389699	29.635612125	43.328799373	1	36.910077853	29.661727430	43.344983974
7	37.492875315	31.545548974	42.763542597	7	37.551669485	31.604920947	42.867406941
6	38.620870910	31.468214672	43.755112529	6	38.729312193	31.480641627	43.793621901
6	37.030714761	32.970815714	42.627759039	6	37.096215263	33.037567619	42.829216785
6	38.014503396	31.087902476	41.426137087	6	38.024886129	31.234573725	41.486587285
1	36.628101375	33.303095031	43.593419219	1	36.746458587	33.322322988	43.830504581
1	37.892488399	33.587868751	42.343479829	1	37.957625044	33.651797136	42.530972742
1	36.255434414	33.017633184	41.843461596	1	36.281794204	33.123387162	42.092464924
1	38.300963398	30.029964039	41.528341762	1	38.301833275	30.170650335	41.509850832
1	37.217960591	31.209008050	40.680620039	1	37.213868130	31.427845333	40.773639933
1	38.876577797	31.705950806	41.137869490	1	38.890528703	31.859750103	41.238204216
1	38.956178877	30.423904919	43.826668512	1	39.099598765	30.447730929	43.758543297
1	39.439330914	32.114595453	43.399839742	1	39.500793089	32.181404377	43.439133846
1	38.248356686	31.795604306	44.734380387	1	38.401732150	31.720788803	44.813535302
8	40.847072087	28.043876911	41.299544670	8	43.162535173	26.833253898	40.348929104
1	40.878077995	27.232415742	41.855678780	1	43.043078108	26.272003550	41.131610503
1	41.068062174	28.790487298	41.895851890	1	43.948602888	27.423630930	40.552273098
8	41.466511036	28.137400365	38.701647335	8	40.841440387	28.189810407	40.433645614
1	41.510453713	28.039639387	39.680479875	1	41.685409327	27.682808527	40.361558988
1	41.890767195	28.995947096	38.528561506	1	40.927436611	28.689184944	41.264944342
1	36.715236140	35.379579708	37.099207988	1	36.574693716	35.504693223	37.098877178
1	39.353454014	29.983930920	32.217309201	1	39.337915983	29.956590983	32.160869654
1	44.304669548	33.449895420	32.693313413	1	44.194429692	33.478335834	32.824279290
1	35.480184188	30.592011868	42.688998748	1	35.547653097	30.646349201	42.794380888

Hydroxylation step

IM2
QM/MM Energy = -3024.059488

6	44.702093616	45.282022276	42.603022997
1	45.320551264	45.788613674	41.848342161
1	45.323792226	45.173047408	43.504347205
6	44.272250297	43.965353349	42.040338081
7	43.691359477	42.946484983	42.770112243
1	43.499207047	42.949583866	43.780945417
6	43.349739626	41.955496897	41.925003249
1	42.848827666	41.038977888	42.224581554
7	43.690274256	42.274875592	40.684255942
6	44.273531393	43.518614565	40.737363827
1	44.652783070	44.018281895	39.849840636
6	42.720594154	43.913368643	35.512280461
1	41.799642899	44.292585632	35.965038286
1	42.456957233	43.451806905	34.547243518
6	43.359829878	42.841107610	36.397384502
8	42.713527838	42.627351159	37.510117350
8	44.384342967	42.263337887	36.040061407
6	38.150324420	43.037510529	41.801069413
1	37.861305011	42.040619201	42.166464107
1	37.253911475	43.454153616	41.311447306
6	39.273796671	42.915503475	40.816122520
7	39.545673665	43.860403472	39.839480652
1	38.991201447	44.680920530	39.601889725
6	40.618106643	43.460476755	39.134961109
1	41.034127518	44.004689300	38.293296889
7	41.062606774	42.295973365	39.591036554
6	40.231741035	41.942820271	40.636208283
1	40.364557132	41.007689294	41.174113253
26	42.862184290	41.357090045	38.969447759
6	42.463684320	38.508157632	39.573492375
6	44.367039204	37.388893436	40.814049696
6	44.811129964	36.587391457	42.060548429
8	42.203241566	39.781447905	39.799313458
8	44.219598426	35.499279184	42.275040034
6	42.857604764	37.703541016	40.806619963
8	45.730728266	37.080157210	42.761228093
1	44.592570785	36.784035035	39.918115751
1	44.961768533	38.312645192	40.752873732
1	42.578893065	38.258978570	41.713993312
1	42.298766368	36.756483876	40.792821158
8	42.407929258	37.986758569	38.467628815
8	44.262428101	40.684127326	38.481998766
6	47.843439216	39.429657749	35.796977688
1	47.506821128	40.271536186	36.419532152
1	48.288902328	39.846775265	34.879069473
7	46.592375134	38.656611510	35.374946688
6	46.952679857	37.514407511	34.473343767
6	45.682153170	39.597226059	34.629855569
6	45.811806465	38.116926002	36.546204507
1	44.778290335	39.044313888	34.338420698
1	45.388654566	40.418851475	35.295059979
1	46.201540116	40.003602129	33.747549854

TS_HAT
QM/MM Energy = -3024.018230

6	44.694188920	45.197354212	42.465583807
1	45.289466493	45.714789574	41.698916545
1	45.335786044	45.099295805	43.355063859
6	44.287003204	43.869027653	41.908948545
7	43.753155145	42.827991163	42.647489571
1	43.562942632	42.835203717	43.659457042
6	43.467510320	41.812629793	41.811082949
1	43.010061009	40.874415411	42.114277171
7	43.798331319	42.134097526	40.564770826
6	44.312907065	43.410989543	40.611018753
1	44.668548081	43.922225588	39.721790605
6	42.767289442	43.946088037	35.501184545
1	41.832324087	44.272799213	35.967493494
1	42.509104106	43.476525902	34.538170954
6	43.482066896	42.915234145	36.379074154
8	42.832693681	42.554046976	37.431991055
8	44.611402838	42.508774450	36.056349652
6	38.181819246	42.971072680	41.743443497
1	37.895239835	41.975113450	42.113559300
1	37.284365308	43.382594765	41.251081829
6	39.304766923	42.844479840	40.758014810
7	39.573064075	43.782347118	39.774443980
1	39.013047016	44.596903355	39.532086409
6	40.640940774	43.372186140	39.065710313
1	41.052051302	43.914192418	38.219787200
7	41.084812861	42.208793636	39.521855338
6	40.259260909	41.868347246	40.575772638
1	40.393054645	40.937559312	41.121426715
26	42.939658210	41.187594609	38.883428827
6	42.375301236	38.357825118	39.559970669
6	44.347401442	37.427566260	40.850246627
6	44.831697131	36.594657801	42.061264660
8	42.217764984	39.644059892	39.777222997
8	44.263146374	35.491308298	42.256571811
6	42.813698594	37.553359116	40.774044325
8	45.763853343	37.083336925	42.747552221
1	44.703895036	36.925155394	39.933051377
1	44.828965571	38.417732168	40.891511376
1	42.428779386	38.032622652	41.686259207
1	42.376043058	36.549522988	40.698845666
8	42.212614491	37.827040244	38.465713934
8	44.297378904	40.278804054	38.180883692
6	47.683073697	39.384774555	35.934559211
1	47.479378451	40.353657637	36.411496776
1	48.082251289	39.586067669	34.928528834
7	46.334116416	38.687808763	35.739051608
6	46.515699721	37.329169788	35.099444396
6	45.492189180	39.546052619	34.826194913
6	45.575053516	38.476130873	37.003826011
1	44.520137289	39.053400692	34.678773751
1	45.334713338	40.520536286	35.305172249
1	46.020594629	39.694108042	33.872941753

1	44.921145718	37.595200801	36.166584136	1	44.693977625	37.843211139	36.832642648
1	46.444415291	37.412231216	37.109348818	1	46.232227496	38.136790733	37.811782376
1	45.483345236	38.961466951	37.163790203	1	44.926516941	39.571771141	37.507213886
1	47.448151421	37.915940688	33.580014115	1	47.101150499	37.456232310	34.178963469
1	47.633475088	36.841203910	35.011220807	1	47.045887789	36.680211919	35.811061725
1	46.047745957	36.959115005	34.192598594	1	45.528158379	36.909066839	34.869225924
8	46.667292059	39.783340307	39.497928780	8	46.590143017	40.398994172	39.702440239
1	46.533298394	38.934573464	39.056196716	1	45.719715807	40.117982262	39.358662737
1	45.880608704	40.302448493	39.217603768	1	46.612701366	41.301976589	39.307952888
8	46.687062502	42.456091494	37.611240703	8	46.531821164	42.552321070	37.999546476
1	46.683074178	43.333084265	38.052747078	1	46.595137804	43.509854252	38.236733096
1	45.757794295	42.264515159	37.380694607	1	45.744034210	42.453166419	37.412561899
1	43.372409977	44.754314552	35.275608910	1	43.373377286	44.820364948	35.263771961
1	43.878544726	45.939401387	42.881747322	1	43.872852652	45.848851502	42.763954948
1	38.344922157	43.686484876	42.654902730	1	38.370394294	43.624418719	42.595291919
1	48.599591758	38.870431753	36.347946774	1	48.444939146	38.858249875	36.509363636

IM3
QM/MM Energy = -3024.048423

6	44.640479059	45.217346264	42.546807270	6	44.687455398	45.199747713	42.469591483
1	45.251353665	45.711370893	41.776929950	1	45.290227566	45.714493637	41.706833899
1	45.280314637	45.101412895	43.435122889	1	45.325041380	45.094974438	43.361292566
6	44.175458651	43.903890004	42.000742007	6	44.272614229	43.875301203	41.908807393
7	43.600193339	42.896678852	42.753889293	7	43.718198299	42.841084797	42.641717586
1	43.432465054	42.911124798	43.769260221	1	43.518367450	42.849673100	43.651819173
6	43.232040965	41.900888191	41.928943423	6	43.435949120	41.826657990	41.803189212
1	42.733225969	40.989075421	42.246950221	1	42.970411399	40.891466005	42.104473718
7	43.546978280	42.201864933	40.674810224	7	43.785514556	42.140511752	40.560011712
6	44.141611691	43.444067312	40.703186983	6	44.311235706	43.413720013	40.612288355
1	44.508227150	43.928997247	39.802393053	1	44.693679354	43.915520060	39.728213759
6	42.687842919	43.982159018	35.516748775	6	42.803597849	44.012168353	35.455283991
1	41.748981168	44.362638185	35.930355306	1	41.861524495	44.350306402	35.897703609
1	42.459644263	43.499929517	34.552447188	1	42.565944817	43.553098231	34.482102714
6	43.284115911	42.938577011	36.458888451	6	43.450351996	42.961741311	36.353348372
8	42.613069025	42.692739735	37.516116119	8	42.787137410	42.612763330	37.378555958
8	44.369707173	42.379658371	36.156861472	8	44.581846320	42.491355347	36.050189986
6	38.006927133	43.115738966	41.899271264	6	38.163259661	42.991400235	41.735459033
1	37.706634211	42.127089457	42.277115186	1	37.875012405	41.995249036	42.103823788
1	37.100978345	43.557886793	41.451953862	1	37.263406888	43.408840565	41.252367995
6	39.079887347	42.962670419	40.865953851	6	39.276644037	42.863341574	40.739366138
7	39.350799036	43.901255431	39.882283498	7	39.545591589	43.808401133	39.763279340
1	38.828522983	44.749610108	39.673293802	1	38.995439336	44.634457821	39.538380666
6	40.380278512	43.462072314	39.136871714	6	40.600595945	43.392933015	39.037875161
1	40.786645104	43.996639033	38.283751722	1	41.008263901	43.939758776	38.193499161
7	40.797914103	42.280642714	39.572072709	7	41.037755293	42.220331245	39.475528352
6	39.992108796	41.956460132	40.646497955	6	40.218812320	41.879058704	40.535414501
1	40.112921909	41.018218074	41.183144043	1	40.346479024	40.942357245	41.073698911
26	42.638225604	41.256039998	39.025893746	26	42.906567555	41.178004176	38.885624495
6	42.209215274	38.375429755	39.665828291	6	42.408366411	38.256778928	39.499420229
6	44.261437889	37.435827383	40.840764045	6	44.366152054	37.358137988	40.815072453
6	44.792373117	36.618113450	42.042602647	6	44.850422618	36.553405090	42.043075737
8	42.051771887	39.661585925	39.909210587	8	42.352627833	39.546338597	39.712916488
8	44.256162886	35.499851018	42.249902982	8	44.285012889	35.451369741	42.255550499
6	42.725400480	37.560328063	40.841194748	6	42.832258062	37.436820014	40.705093815
8	45.719554540	37.132428285	42.717413164	8	45.777322132	37.061164234	42.722782725
1	44.573467661	36.925060385	39.912297453	1	44.759727559	36.859370766	39.910776957
1	44.741556814	38.427754446	40.846838376	1	44.811715916	38.366106445	40.852234354

TS_Rb
QM/MM Energy = -3024.031138

1	42.388055879	38.028331004	41.777683774	1	42.414813875	37.895882674	41.614027878
1	42.287899253	36.555347012	40.776089235	1	42.420552029	36.425297321	40.606812392
8	41.979204800	37.856742084	38.580634595	8	42.180481431	37.731674333	38.410750717
8	44.056105913	40.419124842	38.154265055	8	44.412765611	40.391526524	37.861642763
6	48.087947570	39.173037100	35.584142488	6	47.605931751	39.347656792	35.908390783
1	47.951850839	40.227923979	35.873380146	1	47.467682977	40.363084130	36.307287144
1	48.491931758	39.155935589	34.562608333	1	47.968391575	39.443405483	34.874188421
7	46.697646819	38.544460552	35.532111119	7	46.216963252	38.704064866	35.834579410
6	46.745363081	37.110731891	35.058037663	6	46.288430380	37.260339729	35.364232198
6	45.850401208	39.345390458	34.565202736	6	45.396749560	39.477676261	34.831173539
6	46.029739463	38.582557535	36.834231995	6	45.501037722	38.692323888	37.133883100
1	44.863372712	38.868696951	34.493470611	1	44.382352784	39.054510567	34.797354583
1	45.735912541	40.364173738	34.955183894	1	45.347708429	40.527145678	35.139743053
1	46.353447462	39.391909663	33.588477771	1	45.890978361	39.421036261	33.851953228
1	45.051405069	38.106914794	36.897618100	1	44.574509309	38.117227834	37.102275152
1	46.477633827	39.180956005	37.626925279	1	46.171629584	38.575024406	37.984144598
1	44.312806135	40.897576340	37.339338140	1	44.642790500	41.033850568	37.154241120
1	47.233047341	37.079316622	34.075122541	1	46.848729326	37.230477675	34.419876105
1	47.299169001	36.521348003	35.802618019	1	46.796388997	36.669402066	36.141708688
1	45.717779923	36.733709977	34.976963835	1	45.261671484	36.896916062	35.214059098
8	46.410750262	40.433990019	39.533927142	8	46.547853377	40.542758433	39.638016682
1	45.515350987	40.215136041	39.178549460	1	45.760898957	40.309080867	39.099820131
1	46.498805145	41.337870412	39.151909508	1	46.602764751	41.490948711	39.394352933
8	46.507430633	42.629144435	37.873994014	8	46.541304073	42.798426972	37.982786078
1	46.593390927	43.565583094	38.183883963	1	46.667239056	43.747014027	38.240440089
1	45.687960880	42.582361076	37.330745381	1	45.791719806	42.775194514	37.349813045
1	43.338207102	44.826492762	35.288288103	1	43.427994189	44.879369376	35.240437737
1	43.837314251	45.891564737	42.844167424	1	43.869844412	45.856298920	42.767114777
1	38.262346556	43.757006825	42.742837368	1	38.361037848	43.640542522	42.588433480
1	48.796171994	38.706642080	36.268949892	1	48.368821778	38.836472311	36.495550512

PD

QM/MM Energy = -3024.142064

6	44.627204653	45.209746808	42.441729020
1	45.232094799	45.725594781	41.680529376
1	45.275627306	45.071535569	43.320840018
6	44.160623352	43.909794860	41.861961807
7	43.681547975	42.844553707	42.599309639
1	43.555929170	42.820444455	43.619953405
6	43.314656963	41.869147680	41.737414126
1	42.903537973	40.911145879	42.046836796
7	43.527773866	42.237999283	40.483439902
6	44.059128955	43.504668744	40.547353687
1	44.331916361	44.054856293	39.651016297
6	42.742901160	44.005551219	35.411323639
1	41.818580978	44.336962404	35.894377423
1	42.484515996	43.572212018	34.432302304
6	43.428755595	42.942570675	36.266016388
8	42.915882922	42.694567423	37.395101167
8	44.474780761	42.385683657	35.823775526
6	37.978074114	43.168355985	41.843726597
1	37.663107646	42.177865183	42.204464490
1	37.078317663	43.631667167	41.405017824
6	39.044205518	43.011128709	40.803412683
7	39.354101171	43.962403080	39.846686877
1	38.885484512	44.850698346	39.676680880
6	40.351928878	43.487116342	39.075486820

1	40.779494178	44.033487094	38.238399126
7	40.707652123	42.271260867	39.465474270
6	39.901461802	41.965344378	40.543363616
1	39.979417369	41.017925577	41.073500422
26	42.476159689	41.265084537	38.783269338
6	42.579452273	38.305335386	39.504081407
6	44.493385479	37.239153600	40.814592838
6	44.896277245	36.435739677	42.065445107
8	43.024779874	39.537357702	39.584971283
8	44.281558102	35.358504309	42.273248398
6	42.975845605	37.415536611	40.669206062
8	45.812928945	36.921105399	42.776636961
1	44.878945002	36.709792742	39.925261253
1	44.994989921	38.214005124	40.851666473
1	42.573833935	37.884058590	41.584843001
1	42.484100507	36.443235721	40.553642281
8	41.885451006	37.888451745	38.576479204
8	45.042860782	39.799576856	36.274370514
6	48.432397513	38.780735600	35.161009052
1	48.689272464	39.794592732	34.818749442
1	48.755310266	38.073623538	34.383595025
7	46.921571744	38.701644361	35.236763971
6	46.419623639	37.316449150	35.547359366
6	46.359755208	39.118806751	33.916560431
6	46.399961608	39.683255595	36.327260500
1	45.268764438	39.030647864	33.966710982
1	46.636686304	40.158177291	33.684727974
1	46.768578738	38.460707393	33.138182513
1	46.725470250	39.243295604	37.283722347
1	46.940288251	40.628005650	36.143392271
1	44.789505130	40.723408804	36.023886786
1	46.670519061	36.647358611	34.712139520
1	46.885084433	36.956503415	36.478237251
1	45.328452579	37.367555988	35.667434923
8	45.967062746	40.128262588	39.680463212
1	45.026178491	39.872137112	39.615234522
1	45.995130546	41.020329756	39.284863456
8	46.313621916	42.430381846	37.981285262
1	46.391585341	43.369666679	38.281463999
1	45.569368004	42.413236069	37.339223118
1	43.360456296	44.877610454	35.196368607
1	43.830209629	45.879371604	42.764945494
1	38.241389718	43.789303947	42.699971799
1	48.984892196	38.545462295	36.070659218

References

(1) (a) S. S. Ng, K. L. Kavanagh, M. A. McDonough, D. Butler, E. S. Pilka, B. M. R. Lienard, J. E. Bray, P. Savitsky, O. Gileadi, F. Von Delft, N. R. Rose, J. Offer, J. C. Scheinost, T. Borowski, M. Sundstrom, C. J. Schofield, and U. Oppermann, *Nature* 2007, **448**, 87–91. (b) J. R. Horton, A.

K. Upadhyay, H. H. Qi, X. Zhang, Y. Shi and X. Cheng, *Nat. Struct. Mol. Biol.* 2010, **17**, 38–44.

(c) A. Kawamura, M. Münzel, T. Kojima, C. Yapp, B. Bhushan, Y. Goto, A. Tumber, T. Katoh, O. N. F. King, T. Passioura, L. J. Walport, S. B. Hatch, S. Madden, S. Müller, P. E. Brennan, R. Chowdhury, R. J. Hopkinson, H. Suga and C. J. Schofield, *Nat. Commun.* 2017, **8**, 14773.

(2) R. Salomon-Ferrer, A. W. Götz, D. Poole, S. Le Grand and R. C. Walker, *J. Chem. Theory Comput.* 2013, **9**, 3878–3888.

(3) P. Li and K. M. Merz, *J. Chem. Inf. Model.* 2016, **56**, 599–604.

(4) (a) T. Borowski, A. Bassan and P. E. M. Siegbahn, *Chem. - A Eur. J.* 2004, **10**, 1031–1041.

(b) A. Wójcik, M. Radoń, and T. Borowski, *J. Phys. Chem. A* 2016, **120**, 1261–1274.

(5) A. Pabis, I. Geronimo, D. M. York, and P. Paneth, *J. Chem. Theory Comput.* 2014, **10**, 2246–2254.

(6) M. B. Peters, Y. Yang, B. Wang, L. Füsti-Molnár, M. N. Weaver and K. M. Merz, *J. Chem. Theory Comput.* 2010, **6**, 2935–2947.

(7) J. A. Maier, C. Martinez, K. Kasavajhala, L. Wickstrom, K. E. Hauser and C. Simmerling, *J. Chem. Theory Comput.* 2015, **11**, 3696–3713.

(8) W. L. Jorgensen, J. Chandrasekhar, J. D. Madura, R. W. Impey and M. L. Klein, *J. Chem. Phys.* 1983, **79**, 926–935.

(9) T. Darden, D. York and L. Pedersen, *J. Chem. Phys.* 1993, **98**, 10089–10092.

(10) J. A. Lzaguirre, D. P. Catarello, J. M. Wozniak and R. D. Skeel, *J. Chem. Phys.* 2001, **114**, 2090–2098.

(11) H. J. C. Berendsen, J. P. M. Postma, W. F. Van Gunsteren, A. Dinola and J. R. Haak, *J. Chem. Phys.* 1984, **81**, 3684–3690.

(12) J. P. Ryckaert, G. Ciccotti and H. J. C. Berendsen, *J. Comput. Phys.* 1977, **23**, 327–341.

(13) D. R. Roe, and T. E. Cheatham, *J. Chem. Theory Comput.* 2013, **9**, 3084–3095.

(14) W. Humphrey, A. Dalke and K. Schulten, *J. Mol. Graph.* 1996, **14**, 33–38.

(15) E. F. Pettersen, T. D. Goddard, C. C. Huang, G. S. Couch, D. M. Greenblatt, E. C. Meng and T. E. Ferrin, *J. Comput. Chem.* 2004, **25**, 1605–1612.

(16) B. J. Grant, A. P. C. Rodrigues, K. M. ElSawy, J. A. McCammon and L. S. D. Caves, *Bioinformatics* 2006, **22**, 2695–2696.

(17) P. Sherwood, A. H. De Vries, M. F. Guest, G. Schreckenbach, C. R. A. Catlow, S. A. French, A. A. Sokol, S. T. Bromley, W. Thiel, A. J. Turner, S. Billeter, F. Terstegen, S. Thiel, J. Kendrick, S. C. Rogers, J. Casci, M. Watson, F. King, E. Karlsen, M. Sjøvoll, A. Fahmi, A. Schäfer and C. Lennartz, *J. Mol. Struct. THEOCHEM* 2003, **632**, 1–28.

(18) S. Metz, J. Kästner, A. A. Sokol, T. W. Keal and P. Sherwood, *Wiley Interdiscip. Rev. Comput. Mol. Sci.* 2014, **4**, 101–110.

(19) R. Ahlrichs, M. Bär, M. Häser, H. Horn and C. Kölmel, *Chem. Phys. Lett.* 1989, **162**, 165–169.

(20) W. Smith and T. R. Forester, *J. Mol. Graph.* 1996, **14**, 136–141.

(21) D. Bakowies and W. Thiel, *J. Phys. Chem.* 1996, **100**, 10580–10594.

(22) A. D. Becke, *J. Chem. Phys.* 1993, **98**, 5648–5652.

(23) A. Schäfer, H. Horn and R. Ahlrichs, *J. Chem. Phys.* 1992, **97**, 2571–2577.

(24) R. Ramanan, K. D. Dubey, B. Wang, D. Mandal and S. Shaik, *J. Am. Chem. Soc.* 2016, **138**, 6786-6797.

(25) J. Kästner, J. M. Carr, T. W. Keal, W. Thiel, A. Wander and P. Sherwood, *J. Phys. Chem. A* 2009, **113**, 11856–11865.

(26) S. R. Billeter, A. J. Turner and W. Thiel, *Phys. Chem. Chem. Phys.* 2000, **2**, 2177–2186.

(27) A. J. Mitchell, N. P. Dunham, R. J. Martinie, J. A. Bergman, C. J. Pollock, K. Hu, B. D. Allen, W. C. Chang, A. Silakov, J. M. Bollinger, C. Krebs, A K. Boal, *J. Am. Chem. Soc.* 2017, **139**, 13830–13836.